Preparation, Structure and Properties of Dinuclear, Trinuclear Incomplete Cuboidal and Cuboidal Molybdenum–Selenium Cluster Complexes†

Mohamed Nasreldin,[a] Gerald Henkel,[b] Gunnar Kampmann,[c] Bernt Krebs,[c] Gert J. Lamprecht,[a] Carol A. Routledge[a] and A. Geoffrey Sykes*[,a]

[a] *Department of Chemistry, The University, Newcastle upon Tyne NE1 7RU, UK*

[b] *Fachgebiet Anorganische Chemie der Universität, Lotharstrasse 1, D-4100 Duisburg, Germany*

[c] *Anorganisch-Chemisches Institut der Universität, Wilhelm-Klemm-Strasse 8, D-4400, Münster, Germany*

Preparation of the di-μ-selenido-dimolybdenum(V) complex $[Mo_2O_2(\mu\text{-}Se)_2(cys)_2]^{2-}$ (cys = L-cysteinate dianion), and the related aqua ion $[Mo_2O_2(\mu\text{-}Se)_2(H_2O)_6]^{2+}$, has enabled the trimolybdenum(IV) incomplete cuboidal $Mo_3O_xSe_{4-x}^{4+}$ (x = 0–3) complexes $[Mo_3(\mu_3\text{-}Se)(\mu\text{-}Se)_3(H_2O)_9]^{4+}$ $[Mo_3(\mu_3\text{-}Se)(\mu\text{-}O)(\mu\text{-}Se)_2(H_2O)_9]^{4+}$, $[Mo_3(\mu_3\text{-}Se)(\mu\text{-}O)_2(\mu\text{-}Se)(H_2O)_9]^{4+}$, $[Mo_3(\mu_3\text{-}Se)(\mu\text{-}O)_3(H_2O)_9]^{4+}$ and the mixed-valence (average oxidation state 3.25) cuboidal $[Mo_4(\mu_3\text{-}Se)_4(H_2O)_{12}]^{5+}$ complex to be obtained for the first time. The crystal structures of $Na[NMe_4][Mo_2O_2(\mu\text{-}Se)_2(cys)_2]\cdot 7H_2O$, $[NMe_4]_5[Mo_3(\mu_3\text{-}Se)(\mu\text{-}Se)_3(NCS)_9]$, $[NMe_4]_5[Mo_3(\mu_3\text{-}Se)(\mu\text{-}O)_2(\mu\text{-}Se)(NCS)_9]$ and $[Mo_4Se_4(H_2O)_{12}](pts)_5\cdot 14H_2O$ (pts^- = toluene-*p*-sulfonate) have been determined. Electrolytic reduction of $[Mo_4(\mu_3\text{-}Se)_4(H_2O)_{12}]^{5+}$ in 2 M Hpts gives quantitatively the air-sensitive tetramolybdenum(III) analogue $[Mo_4(\mu_3\text{-}Se)_4(H_2O)_{12}]^{4+}$ (E_f° = 190 mV). Similarly the 5+ ion can be oxidised to the 6+ state (E_f° = 790 mV). Compared to analogous Mo–S clusters, Mo–Se clusters exhibit identical structures but with longer bond distances, red-shifted absorption bands, and in the case of the cuboidal aqua complexes less-positive reduction potentials. By analogy with $[Mo_3S_4(H_2O)_9]^{4+}$, $[Mo_3MSe_4(H_2O)_{10}]^{4+}$ hetero-metal cuboidal and related complexes are obtained. The edta(=*N,N,N',N'*-ethylenediamine-tetraacetate) complex of the 5+ cube $[Mo_4Se_4(edta)_2]^{3-}$ has been prepared, and reduction potentials for the corresponding core 5+/4+ and 6+/5+couples determined as −40 and 650 mV respectively.

The study of Mo–S cuboidal and incomplete cuboidal clusters has provided valuable insight into the properties of this type of co-ordination complex. The present paper reports on the preparation and characterisation of related Mo–Se clusters. In a recent paper Holm and co-workers[1] have described synthetic studies and the binuclear Fe_2Se_2 and cuboidal Fe_4Se_4 clusters with thiolate ligands. Other reports on the preparation of selenium cluster analogues have appeared.[2–4] It has also been established that ferredoxin apoproteins can be reconstituted with Fe^{II}/Fe^{III} and a selenide source to yield holoproteins containing Fe_2Se_2 and Fe_4Se_4 clusters.[5] Although there is no evidence for the inclusion of selenide in metal clusters in biology, comparisons of Se with S in Fe_2Se_2 and Fe_4Se_4 have proved instructive. Selenium is known to have a biological role in selenocysteine.[6] In the case of the Mo–S clusters, Mo as an early transition metal has a higher co-ordination number of six.[7,8] The increased stability of the aqua ions in aqueous (acidic) solutions has enabled a whole range of studies not possible in the case of the Fe–S clusters.[9,10] A particular interest has been the metal-depleted or incomplete cuboidal $Mo_3S_4^{4+}$ cluster,[11] and related trinuclear forms with oxosulfido cores, $Mo_3O_xS_{4-x}^{4+}$ (x = 0–4).[1,12] Although the $Fe_3S_4^+$ incomplete cube has been identified in about 20 proteins,[13] there are as yet no synthetic analogues, and only linear trinuclear $Fe(\mu\text{-}S)_2Fe(\mu\text{-}S)_2Fe^+$ forms have been synthesised.[14] In both cases the incomplete cubes have higher (average) metal oxidation states than do the corresponding cubes.

To prepare the Mo–Se clusters, the lead-in complex is the di-μ-selenido-dimolybdenum(V) complex $[Mo_2O_2(\mu\text{-}Se)_2(cys)_2]^{2-}$ **1** [cys = cysteinate(2−)‡]. From this the aqua ion $[Mo_2O_2(\mu\text{-}Se)_2(H_2O)_6]^{2+}$ **2**, trimolybdenum(IV) $[Mo_3(\mu_3\text{-}Se)(\mu\text{-}Se)_3(H_2O)_9]^{4+}$ **3**, and mixed-valence (average oxidation state 3.25) $[Mo_4(\mu_3\text{-}Se)_4(H_2O)_{12}]^{5+}$ **7** have now been obtained, as well as related trinuclear aqua ions, $[Mo_3(\mu_3\text{-}Se)(\mu\text{-}O)(\mu\text{-}Se)_2(H_2O)_9]^{4+}$ **4**, $[Mo_3(\mu_3\text{-}Se)(\mu\text{-}O)_2(\mu\text{-}Se)(H_2O)_9]^{4+}$ **5**, and $[Mo_3(\mu_3\text{-}Se)(\mu\text{-}O)_3(H_2O)_9]^{4+}$ **6**, Fig. 1. Four of these have been characterised by X-ray analysis. A communication describing the initial findings has appeared.[15] It has also been found that the $Mo_3Se_4^{4+}$ ion can be converted into mixed-metal cuboidal complexes of the kind $Mo_3MSe_4^{4+}$, with the potential to open up a whole new area of heterometal cluster chemistry.[16,17]

Experimental

Preparation of Compounds.—The caesium salt of di-μ-selenido-bis[cysteinatooxomolybdate(V)] **1** is the lead-in complex to the aqua ions **2**–**7**. Of these **3**–**5** and **7** are obtained in one and the same procedure, and have to be separated by Dowex 50W-X2 cation-exchange chromatography. Alternative procedures are given for **5** and **6**, and **5** can also be converted into **6**. Electrochemical reduction of **7** to the tetramolybdenum(III) 4+ cube, and preparation of **7** as the *N,N,N',N'*-ethylenediamine-tetraacetate (edta) complex **8**, are also described. Air-free techniques employed N_2 gas, rubber seals, Atlas nylon syringes and Teflon needles.

The following procedure was used to prepare $[Mo_2O_2Se_2$-

† *Supplementary data available:* see Instructions for Authors, *J. Chem. Soc., Dalton Trans.*, 1993, Issue 1, pp. xxiii–xxviii.

Non-SI unit employed: M = mol dm^{-3}.

‡ Cysteinate here refers to the doubly deprotonated form of cysteine (Cys).

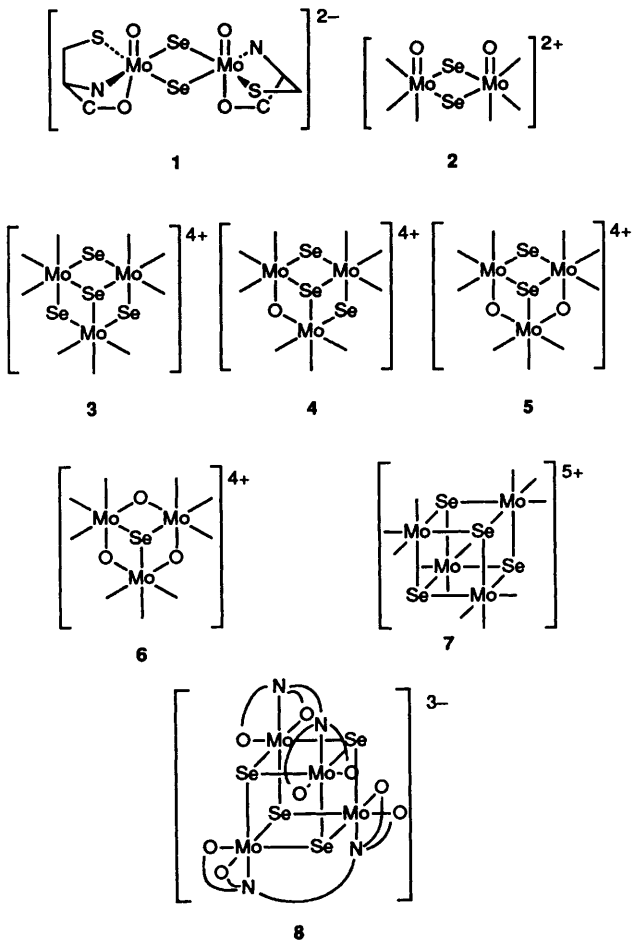

Fig. 1 Schematic structural formulae of the Mo–Se cluster complexes **1**–**8**; water as ligands unless otherwise indicated.

$(cys)_2]^{2-}$ **1**. To a solution of heptamolybdate(VI), $[NH_4]_6[Mo_7O_{24}]\cdot 6H_2O$ (2.47 g, 2.0 mmol), in water (50 cm^3), freshly prepared NaHSe (2.16 g, 21 mol) in water (30 cm^3) was added slowly. The deep black reaction mixture was stirred for 24 h, and a dark precipitate removed by filtering. A solution of L(+)-cysteine hydrochloride monohydrate (2.46 g, 14.0 mmol) in water (20 cm^3), pH adjusted to ≈ 6 with sodium hydroxide, was added dropwise to the filtered reaction mixture. After standing for 24 h at ambient temperature, the mixture was re-filtered. On addition of caesium chloride (20 mmol) in water (20 cm^3), crystals of $Cs_2[Mo_2O_2(\mu\text{-}Se)_2(cys)_2]\cdot 4H_2O$ separated within 24 h. Recrystallisation was from hot water, yield 33.7% (Found: C, 7.50; H, 2.05; N, 2.85. Calc. for $C_6H_{18}Cs_2Mo_2N_2O_{10}S_2Se_2$: C, 7.50; H, 1.90; N, 2.90%). UV/VIS: λ/nm (ε/M^{-1} cm^{-1} per dinuclear complex) 205 (sh) (39 500), 237 (31 900), 304 (9280) and 394 (3460). Crystals of $Na[NMe_4][Mo_2O_2Se_2(cys)_2]\cdot 7H_2O$ were used in an X-ray diffraction study. On addition of 2 M $HClO_4$ and leaving to stand for ≈ 15 min to remove the cysteine ligands, the aqua ion $[Mo_2O_2(\mu\text{-}Se)_2(H_2O)_6]^{2+}$ **2** is obtained, Fig. 2.

Trinuclear and cube complexes were obtained as follows. The procedure for the preparation of $[Mo_4Se_4(H_2O)_{12}]^{5+}$ **7** and $[Mo_3O_xSe_{4-x}(H_2O)_9]^{4+}$ **3**–**5** (x = 0–2) is described first. To a solution of $Cs_2[Mo_2O_2Se_2(cys)_2]\cdot 4H_2O$ (2 g, 2 mmol) in 0.03 M HCl (400 cm^3) under N_2 was added $NaBH_4$ (1 g, 30 mmol). After 30 min concentrated HCl (60 cm^3) was added slowly with stirring to give a final HCl concentration of 1.5 M, and the solution left air-free overnight at ≈ 4 °C. It was then heated in air at 90 °C for 2 h. After filtration and five-fold dilution with water the products were loaded onto a Dowex 50W-X2 cation-exchange column (30 × 1.5 cm diameter) and washed first with

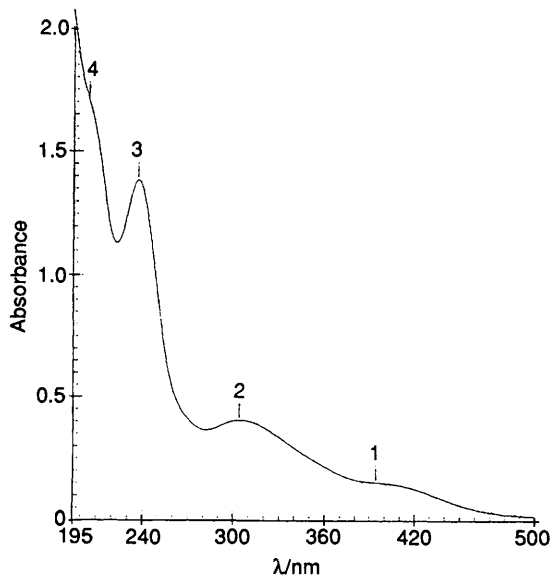

Fig. 2 The UV/VIS absorption spectrum of the dimolybdenum(V) complex $[Mo_2O_2Se_2(cys)_2]^{2-}$ (2.15×10^{-4} M) in water, in a 2 mm pathlength cell; ε values per dinuclear complex are given in the text

0.5 HCl (≈ 100 cm^3) and then 1.0 M HCl (≈ 150 cm^3). The first (green) band, corresponding to $[Mo_3O_2Se_2(H_2O)_9]^{4+}$, was followed by the yellow-brown $[Mo_3OSe_3(H_2O)_9]^{4+}$ on elution with 1.5 M HCl. The third band corresponding to $[Mo_3Se_4(H_2O)_9]^{4+}$, and the fourth green band, $[Mo_4Se_4(H_2O)_{12}]^{5+}$, were eluted with 2.0 M HCl. Red elemental Se was retained at the top of the column. Purification of each band was carried out on a separate Dowex 50W-X2 cation-exchange column. The total yield of cube and trinuclear products was $\approx 10\%$.

An alternative procedure involving reduction of the dinuclear molybdenum(V) ion $[Mo_2O_2Se_2(H_2O)_6]^{2+}$ with $[MoCl_6]^{3-}$ gives $[Mo_3O_2Se_2(H_2O)_9]^{4+}$ in high yield (> 70%). The procedure involves heating (with a reflux condenser in place) a solution of 2:1 molar ratio of $K_3[MoCl_6]$ and $[Mo_2O_2Se_2(H_2O)_6]^{2+}$ in 1 M HCl under N_2 for 1 h on a steam-bath at ≈ 90 °C. The same procedure has been used for $[Mo_3O_2S_2]^{4+}$.[12]

The trinuclear complex $[Mo_3O_2Se_2(H_2O)_9]^{4+}$ **5** (2 mM), in 0.5 M $HClO_4$ (50 cm^3) was converted into $[Mo_3O_3Se(H_2O)_9]^{4+}$ **6** by treating with a 30-fold excess of $NaBH_4$ (0.19 g), using a procedure successfully applied to the Mo–S analogue.[18] The resulting solution was filtered and loaded onto a Dowex column (20 × 1 cm). After washing with 0.5 (50) and 1.0 M (50 cm^3) HCl brown-red **6** was eluted.

A second procedure was used to prepare $[Mo_3O_3Se(H_2O)_9]^{4+}$. Thus the di-μ-oxo-bis(L-cysteinatooxomolybdate(V)] complex $Na_2[Mo_2O_4(cys)_2]$ was first prepared by sodium dithionite reduction of a solution of sodium molybdate(VI), $Na_2[MoO_4]\cdot 2H_2O$ in the presence of cysteine.[19] To a solution of this dimolybdenum(V) complex (2 g in 100 cm^3 water), grey selenium powder (2 g) was added, and the suspension transferred to an electrochemical cell as in ref. 1. After reduction at −0.9 V (*vs.* normal hydrogen electrode, NHE) for 8–10 h concentrated HCl was added to give $[H^+] = 0.5$ M, and the reduction continued for 36 h. The suspension was diluted by addition of 0.5 M HCl (0.5 l) and left to air-oxidise for 12 h. After filtering, the brown-yellow solution was diluted to $[H^+] \approx 0.3$ M and loaded onto a Dowex 50W-X2 cation-exchange column. The column was washed with 0.5 M HCl (200 cm^3), when some yellow material was obtained, and elution commenced with 1.0 M HCl. Two clearly defined red bands were collected. The first, a Se-containing product, was browner than the second which was predominantly $[Mo_3O_4(H_2O)_9]^{4+}$. The former was diluted to 0.3 M HCl and recolumned. Further yellow material obtained on washing with

Table 1 Results of analyses by ICP atomic emission spectroscopy on 2 M Hpts solutions

Origin	Amount (ppm) Mo	Se	Mo/Se[a]	Formula
Band 1	211	117	1.48 (1.50)	**5** $Mo_3O_2Se_2^{4+}$
Band 2	115	103	0.93 (1.0)	**4** $Mo_3OSe_3^{4+}$
Band 3	119	133	0.74 (0.75)	**3** $Mo_3Se_4^{4+}$
Band 4	339	295	0.94 (1.0)	**7** $Mo_4Se_4^{5+}$
[b]	—	—	3.11 (3.0)	**6** $Mo_3O_3Se^{4+}$

[a] Calculated ratio in parentheses. [b] Alternative preparative route (see Experimental section).

Table 2 Peak positions λ/nm (ε/M^{-1} cm^{-1} per Mo_2, Mo_3 or Mo_4 unit) in the UV/VIS spectra of Mo–Se cluster complexes (in 2 M Hpts) based on ICP analysis as in Table 1 or as stated

Complex	
2 $[Mo_2O_2Se_2(H_2O)_6]^{2+}$ [a]	247, 303, 330 (sh), 419
3 $[Mo_3Se_4(H_2O)_9]^{4+}$	330 (sh) (1833), 425 (2462), 648 (263)
4 $[Mo_3OSe_3(H_2O)_9]^{4+}$	337 (2440), 440 (sh) (1615), 660 (347)
5 $[Mo_3O_2Se_2(H_2O)_9]^{4+}$	380 (4020), 634 (398)
6 $[Mo_3O_3Se(H_2O)_9]^{4+}$	350 (1880), 525 (184)
7 $[Mo_4Se_4(H_2O)_{12}]^{5+}$	435 (sh) (669), 662 (407), 1188 (117)
$[Mo_4Se_4(H_2O)_{12}]^{4+}$ [b]	403 (1172), 450 (sh), (728)

[a] Solution of cysteinato complex of known concentration aquated to give ε values, in 1 M HCl. [b] Solution air oxidised to relate to known spectrum of complex **7**.

0.5 M HCl was discarded, and a diffuse red band (peaks at 356 and 538 nm) eluted with 1 M HCl. This procedure was repeated using 0.5 M toluene-*p*-sulfonic acid (Hpts) to wash the column, and 2 M Hpts to elute the red product. The overall yield was ≈3%. Attempts to improve the yield using aqua $[Mo_2O_4(H_2O)_9]^{2+}$ instead of the cysteinato complex, and using $NaBH_4$ as reductant, did not in our experience give Se-containing products. We thank Dr. M. Martinez at the University of Barcelona for help with this preparation.

To obtain a solid sample the $Mo_3O_3Se^{4+}$ core was eluted from a cation-exchange column with 1 M NaNCS in 0.5 M HCl. Solid tetramethylammonium bromide was added to the eluate when a green sample was obtained {Found: C, 25.7; H, 4.10; N, 14.6. Calc. for $[NMe_4]_5[Mo_3O_3Se(NCS)_9]$: C, 26.6; H, 4.6; N, 15.0%}. The ratio of Mo to Se was determined by inductively coupled plasma (ICP) atomic emission spectroscopy, which gave for different samples 3.15 : 1 and 3.07 : 1 in accordance with the above formula. Analyses for Mo and Se in the other trinuclear complexes were likewise obtained for the different eluted fractions. These gave Mo/Se ratios, Table 1, consistent with the formulae indicated. Absorption coefficients (ε) at different UV/VIS peak positions were based on these analyses, Table 2.

To obtain crystals, solutions of the trinuclear ions $[Mo_3Se_4(H_2O)_9]^{4+}$, $[Mo_3O_2Se_2(H_2O)_9]^{4+}$ and $[Mo_3O_3Se(H_2O)_9]^{4+}$ in 2 M HCl were diluted eight times and loaded onto a narrow Dowex 50W-X2 cation-exchange column (12 × 0.6 cm diameter). After washing with 0.5 M HCl, slow elution with NCS^- (1 M) in 0.25 M HCl was carried out. Upon addition of solid tetramethylammonium bromide (Aldrich, Reagent Grade), a precipitate was immediately formed. A solution of NCS^- (1 M) in 0.25 M HCl was added dropwise while heating to ≈60 °C with continuous stirring until all the precipitate dissolved. The resultant solution was then filtered and left to stand at room temperature. Crystals of the thiocyanato derivatives $[NMe_4]_5[Mo_3Se_4(NCS)_9]$ and $[NMe_4]_5[Mo_3O_2Se_2(NCS)_9]$ separated after ≈10 d.

Solutions of $[Mo_4Se_4(H_2O)_{12}]^{5+}$ in HCl were diluted to ≈0.5 M H^+ and loaded onto Dowex 50W-X2 column (10 × 1.2 cm diameter) under N_2. After washing with 0.5 (50) and 1.0 M Hpts (50 cm^3), elution was with 4 M Hpts. Crystals of $[Mo_4Se_4(H_2O)_{12}][MeC_6H_4SO_3]_5 \cdot 14H_2O$ were obtained after keeping at 4 °C under N_2 for a few days.

To prepare $[Mo_4Se_4(H_2O)_{12}]^{4+}$, a solution of $[Mo_4Se_4(H_2O)_{12}]^{5+}$ (50 cm^3, 1.0 mM) in 2 M Hpts was electrochemically reduced under N_2 using a carbon-cloth (RGV1000, Le Carbonne, Brighton) electrode at a potential of −0.15 V (*vs.* saturated calomel electrode, SCE) for 2 h. The latter potential was selected following cyclic voltammetry experiments (see below). After reduction was complete the yellowish brown solution of $[Mo_4Se_4(H_2O)_{12}]^{4+}$ was Millipore filtered (pore size 8 μm) to remove any small carbon particles. Details of the UV/VIS absorption spectrum are given in Table 2.

Oxygen was bubbled through a sample of $[Mo_4Se_4(H_2O)_{12}]^{4+}$ (3 cm^3, 1.0 mM) in 2 M Hpts for 2 min, then the cell was stoppered and placed in a spectrophotometer at 25 °C. The formation of $[Mo_4Se_4(H_2O)_{12}]^{5+}$ was complete within 5 min.

To obtain $[Mo_4Se_4(edta)_2]^{3-}$, the dimolybdenum(v) complex $[Mo_2O_2(\mu\text{-}Se)_2(edta)]^{2-}$ was first prepared from the aqua complex $[Mo_2O_2(\mu\text{-}Se)_2(H_2O)_6]^{2+}$. The procedure used was to take $[Mo_2O_2Se_2(H_2O)_6]^{2+}$ (0.01 M) in 1 M HCl (≈200 cm^3) and add disodium dihydrogen ethylenediaminetetraacetate (BDH, Analar) in a 1 : 1 molar ratio. The pH of the solution was raised to 6 by addition of a saturated solution of sodium hydrogencarbonate (BDH, Analar). A pale orange solid of the sodium salt of $[Mo_2O_2Se_2(edta)]^{2-}$ was obtained within minutes. After leaving to stand overnight, the solid was filtered off.

To convert into the cuboidal complex a solution of the above dimolybdenum(v) solid (1 g) in 0.03 M HCl (100 cm^3) was treated with $NaBH_4$ (0.5 g) under a nitrogen atmosphere. The solution was left overnight at 4 °C after which it was subjected to air oxidation on a steam-bath (≈90 °C) for ≈20 h. The solution changed gradually from an initial dark brown to dark green. Any brown solid formed was filtered off. The filtrate was then loaded onto a Sephadex G10 column and eluted with water. Sufficient 1 M $LiClO_4$ was added to the green solution to give a 0.10 M $LiClO_4$ solution prior to loading onto a QAE-Sephadex anion-exchange column. After washing with 0.1 M $LiClO_4$, $[Mo_4Se_4(edta)_2]^{3-}$ was eluted with 0.25 M $LiClO_4$. Solutions of $[Mo_4Se_4(edta)_2]^{3-}$ in 0.5 M $LiClO_4$ were stable for weeks at ≈4 °C.

X-Ray Structure Determination.—Single crystals of $Na[NMe_4][Mo_2O_2Se_2(cys)_2] \cdot 7H_2O$, $[NMe_4]_5[Mo_3Se_4(NCS)_9]$ and $[Mo_4Se_4(H_2O)_{12}][MeC_6H_4SO_3]_5 \cdot 14H_2O$ suitable for X-ray diffraction were fixed at the top of a glass fibre and cooled to approximately 150 K under a stream of cold nitrogen gas by using a modified Syntex LT-1 cooling device or mounted in a glass capillary in the case of $[NMe_4]_5[Mo_3O_2Se_2(NCS)_9]$ under an atmosphere of pure dinitrogen. Data collections were performed with a Syntax $P2_1$ four-circle diffractometer equipped with molybdenum X-ray tube, a graphite monochromator and scintillation counter. The orientation matrix and the unit-cell dimensions were obtained by a least-squares fit of the setting angles of at least 15 centred reflections in the range $20 < 2\theta < 30$ °C. The intensities of two standard reflections monitored every 98 scans did not show any significant changes during data collection. The intensity profiles of all reflections indicated stable crystal settings during the measurements. All calculations including data reduction (Lorentz and polarisation corrections) and empirical absorption corrections were done by using the SHELXTL+ program package[20] on an MS-DOS personal computer equipped with an Intel 80386 or 80486 microprocessor. The structures were solved by direct methods which revealed the positions of the molybdenum, selenium and sulfur atoms. The remaining non-hydrogen atoms were located from Fourier difference maps computed after least-squares

Table 3 Crystallographic data for $Na[NMe_4][Mo_2O_2Se_2(cys)_2]\cdot 7H_2O$ **a**, $[NMe_4]_5[Mo_3Se_4(NCS)_9]$ **b**, $[NMe_4]_5[Mo_3O_2Se_2(NCS)_9]$ **c** and $[Mo_4Se_4(H_2O)_{12}][MeC_6H_4SO_3]_5\cdot 14H_2O$ **d**

Compound	**a**	**b**	**c**	**d**
Formula	$C_{10}H_{36}Mo_2N_3NaO_{13}S_2Se_2$	$C_{29}H_{60}Mo_3N_{14}S_9Se_4$	$C_{29}H_{60}Mo_3N_{14}O_2S_9Se_2$	$C_{35}H_{87}Mo_4O_{41}S_5Se_4$
M_r	843.33	1497.09	1371.20	2023.98
Space group	$P222_1$ (orthorhombic)	$P2_1/n$ (monoclinic)	$P\bar{1}$ (triclinic)	$P\bar{1}$ (triclinic)
T/K	150	150	295	150
a/Å	19.092(6)	15.313(7)	13.196(3)	12.603(9)
b/Å	12.296(4)	20.484(6)	13.361(4)	16.384(16)
c/Å	24.068(6)	18.658(9)	17.908(6)	16.946(8)
α/°			98.04(4)	90.16(6)
β/°		101.20(7)	90.07(4)	92.91(6)
γ/°			107.79(4)	95.99(6)
U/Å^3	5650	5741	2973	3475
Z	8	4	2	2
D_c/g cm^{-3}	1.983	1.732	1.531	1.934
μ(Mo-Kα)/mm^{-1}	3.6	3.3	2.1	2.9
Scan type	ω–2θ	ω	ω	ω–2θ
No. unique reflections	6797	7106	9399	10 946
No. observed reflections [$I > 3\sigma(I)$]	5245	2580	3165	5147
No. of variables	142	299	318	380
R (R')	0.049 (0.059)	0.085 (0.098)	0.072 (0.067)	0.074 (0.079)

Table 4 Atomic coordinates of the anion (without H atoms) of $Na[NMe_4][Mo_2O_2Se_2(cys)_2]\cdot 7H_2O$

Atom	x	y	z
Mo	0.307 56(5)	0.381 35(8)	0.007 10(10)
Se	0.286 25(6)	0.506 86(14)	0.160 55(9)
S	0.286 9(2)	0.242 4(2)	0.153 9(3)
O(1)	0.394 1(4)	0.362 7(5)	0.001 3(9)
O(2)	0.188 6(4)	0.345 0(6)	−0.016 0(8)
O(3)	0.115 3(4)	0.205 6(7)	−0.027 6(11)
N(1)	0.295 0(5)	0.230 0(8)	−0.096 8(9)
C(1)	0.174 1(6)	0.244 8(9)	−0.027 2(10)
C(2)	0.234 7(6)	0.164 6(9)	−0.046 9(11)
C(3)	0.256 8(7)	0.123 2(11)	0.067 8(11)

refinement cycles. Atomic scattering factors for spherical neutral free atoms (bonded for hydrogen) were taken from standard sources.[21] Both the f' and f'' components of the anomalous dispersion[21] were included for all non-hydrogen atoms. Unless otherwise stated, all non-hydrogen atoms were refined anisotropically during the last stage of the refinement. With the exception of the $MeC_6H_4SO_3^-$ (*i.e.* pts$^-$) counter ions in crystals of $[Mo_4Se_4(H_2O)_{12}][MeC_6H_4SO_3]_5\cdot 14H_2O$, all other hydrogen atoms were neglected. Further details relevant to the data collections and structure refinements are collected in Table 3.

(*a*) $Na[NMe_4][Mo_2O_2Se_2(cys)_2]\cdot 7H_2O$. For the observed Laue symmetry *mmm*, the systematic absences (*hkl*, $l = 2n + 1$) were characteristic for the space group $P222_1$. The reflections *hkl*, $l = 2n + 1$ were very weak thus indicating a systematic relationship between molecules which are not related by symmetry. In addition, the data set obtained by a corresponding transformation of the unit cell ($c' = c/2$) indicates the presence of a pseudo-body-centred lattice because all remaining reflections with odd index sums were again very weak. The structure was initially solved for the body-centred sub-cell in the space group *Immm* and subsequently expanded to meet the requirements of the true supercell. In the course of the lattice expansion, it was found that the $[Mo_2O_2Se_2(cys)_2]^{2-}$ anions and the Na^+ cations can be perfectly described in the orthorhombic subcell by using the symmetry elements of the space group *I*222. The additional reflections which define the orthorhombic supercell originate from the positions of the $[NMe_4]^+$ cations and the water molecules in the lattice. Their spatial distribution was completely determined from a refinement of the structure in the supercell. However, the corresponding structural model suffered from severe correlations between positional and thermal parameters of atoms related by pseudo-inversion centres. The final structural model was therefore derived from the subcell by using a statistical superposition of the $[NMe_4]^+$ cations and the water molecules. The asymmetric unit contains one half-anion. The other half is generated by a two-fold symmetry axis. Final R factors and other details are included in Table 3. Positional parameters of the $[Mo_2O_2Se_2(cys)_2]^{2-}$ anion are listed in Table 4, selected interatomic distances and angles within the anion in Table 9.

(*b*) $[NMe_4]_5[Mo_3Se_4(NCS)_9]$. In combination with the observed Laue symmetry 2/*m*, the systematic absences (*h*0*l*, $h + l = 2n + 1$) were characteristic for the monoclinic space group $P2_1/n$. Besides one $[Mo_3Se_4(NCS)_9]^{5-}$ anion, the asymmetric unit contains five $[NMe_4]^+$ cations. Two of them were severely affected by disorder resulting in large thermal vibrations of the others as well as of the NCS^- ligands. For this reason, only the heavy atoms Mo, Se and S were refined with anisotropic thermal parameters. Final R factors and other details are included in Table 3, positional parameters and selected bond distances and valence angles of the $[Mo_3Se_4(NCS)_9]^{5-}$ anion in Tables 5 and 9.

(*c*) $[NMe_4]_5[Mo_3O_2Se_2(NCS)_9]$. Under the observed Laue symmetry ($\bar{1}$) the distribution of the normalised structure factors indicated the centrosymmetric space group $P\bar{1}$. The successful structure solution and refinement confirmed this choice. The asymmetric unit contains one $[Mo_3O_2Se_2(NCS)_9]^{5-}$ anion and five NMe_4^+ cations. The positional disorder of one cation led to large thermal vibrations of the others as well as of the NCS^- ligands. Consequently, only the heavy atoms Mo, Se and O were refined with anisotropic thermal parameters. Final R factors and other details are included in Table 3, positional parameters and selected bond distances and valence angles of the $[Mo_3O_2Se_2(NCS)_9]^{5-}$ anion in Tables 6 and 11.

(*d*) $[Mo_4Se_4(H_2O)_{12}][MeC_6H_4SO_3]_5\cdot 14H_2O$. Under the given Laue symmetry ($\bar{1}$), the distribution of the normalised structure factors indicated a centrosymmetrical crystal lattice. Assuming the space group $P\bar{1}$, the structure was successfully solved and refined. The asymmetric unit contains one $[Mo_4Se_4(H_2O)_{12}]^{5+}$ cation and five $MeC_6H_4SO_3^-$ anions. The phenyl rings of the anions were refined as idealised hexagons (C–C 1.395 Å) with rigid stereochemistry, the hydrogen atoms within the anions being calculated at ideal positions (C–H 0.96 Å). They were included in the refinements with thermal parameters set to 1.2 times the values of those of the carbon atoms to which they are bonded. The Mo, Se and S

Table 5 Atomic coordinates of the anion of $[NMe_4]_5[Mo_3Se_4(NCS)_9]$

Atom	*x*	*y*	*z*
Mo(1)	0.6526(2)	0.1074(2)	0.5394(2)
Mo(2)	0.5204(2)	0.1092(2)	0.6254(2)
Mo(3)	0.6836(2)	0.0449(2)	0.6762(2)
Se(1)	0.6650(3)	0.1633(2)	0.6572(3)
Se(2)	0.4997(3)	0.0756(2)	0.4999(3)
Se(3)	0.7050(2)	−0.0024(2)	0.5627(3)
Se(4)	0.5369(3)	−0.0020(2)	0.6692(2)
S(1)	0.6286(14)	0.3315(10)	0.4529(12)
S(2)	0.6855(10)	0.0758(9)	0.2829(11)
S(3)	0.9687(9)	0.1591(9)	0.5495(10)
S(4)	0.5290(13)	0.2148(9)	0.8627(10)
S(5)	0.1935(7)	0.1118(7)	0.5804(8)
S(6)	0.3939(8)	0.3284(5)	0.6155(7)
S(7)	0.9782(9)	0.1234(8)	0.7850(9)
S(8)	0.8434(12)	−0.1335(7)	0.8136(9)
S(9)	0.7151(11)	0.0694(8)	0.9400(9)
N(1)	0.626(2)	0.209(2)	0.494(2)
N(2)	0.662(2)	0.086(2)	0.428(2)
N(3)	0.791(2)	0.140(2)	0.550(2)
N(4)	0.508(2)	0.142(2)	0.732(2)
N(5)	0.373(2)	0.095(2)	0.615(2)
N(6)	0.469(2)	0.213(2)	0.601(2)
N(7)	0.818(2)	0.073(2)	0.711(2)
N(8)	0.739(2)	−0.047(2)	0.726(2)
N(9)	0.689(2)	0.063(2)	0.791(2)
C(1)	0.621(3)	0.252(3)	0.476(3)
C(2)	0.672(3)	0.084(2)	0.378(3)
C(3)	0.860(3)	0.151(2)	0.545(3)
C(4)	0.514(3)	0.171(2)	0.783(3)
C(5)	0.299(3)	0.100(2)	0.595(2)
C(6)	0.439(2)	0.263(2)	0.612(2)
C(7)	0.882(3)	0.094(2)	0.735(2)
C(8)	0.779(3)	−0.079(2)	0.769(3)
C(9)	0.702(3)	0.065(2)	0.857(3)

Table 6 Atomic coordinates of the anion of $[NMe_4]_5[Mo_3O_2Se_2(NCS)_9]$

Atom	*x*	*y*	*z*
Mo(1)	0.2264(2)	0.2651(2)	0.2416(1)
Mo(2)	0.2917(2)	0.4721(2)	0.2822(1)
Mo(3)	0.4284(2)	0.3483(2)	0.2859(1)
Se(1)	0.3559(2)	0.3851(2)	0.1690(1)
Se(2)	0.4091(2)	0.4792(2)	0.3883(2)
O(1)	0.1752(10)	0.3602(10)	0.3089(8)
O(2)	0.3139(10)	0.2324(10)	0.3128(7)
S(1)	−0.0308(11)	0.2625(10)	0.0449(6)
S(2)	0.2577(10)	−0.0270(9)	0.0577(6)
S(3)	−0.0294(8)	0.0206(8)	0.3819(6)
S(4)	0.1037(7)	0.6759(8)	0.4450(6)
S(5)	0.5793(7)	0.7935(7)	0.2494(7)
S(6)	0.0603(8)	0.6120(8)	0.1479(7)
S(7)	0.7647(7)	0.5757(7)	0.2078(5)
S(8)	0.5624(10)	0.2043(11)	0.4826(7)
S(9)	0.5937(8)	0.0948(7)	0.1547(6)
N(1)	0.1079(15)	0.2576(14)	0.1622(11)
N(2)	0.2392(14)	0.1357(15)	0.1628(11)
N(3)	0.1015(14)	0.1441(14)	0.2889(10)
N(4)	0.2226(16)	0.5713(16)	0.3601(12)
N(5)	0.4068(16)	0.6209(16)	0.2594(10)
N(6)	0.1926(15)	0.5170(14)	0.2087(10)
N(7)	0.5811(15)	0.4576(14)	0.2614(10)
N(8)	0.5175(14)	0.3065(14)	0.3717(11)
N(9)	0.4907(14)	0.2374(14)	0.2153(10)
C(1)	0.0513(21)	0.2613(19)	0.1158(15)
C(2)	0.2513(18)	0.0695(20)	0.1198(15)
C(3)	0.0477(19)	0.0909(19)	0.3261(14)
C(4)	0.1749(21)	0.6124(20)	0.3983(15)
C(5)	0.4792(21)	0.6900(20)	0.2563(13)
C(6)	0.1361(21)	0.5543(20)	0.1841(14)
C(7)	0.6554(20)	0.5080(18)	0.2367(13)
C(8)	0.5352(20)	0.2654(20)	0.4203(16)
C(9)	0.5337(20)	0.1784(21)	0.1903(14)

Table 7 Atomic coordinates of the cation (without H atoms) of $[Mo_4Se_4(H_2O)_{12}][MeC_6H_4SO_3]_5\cdot 14H_2O$

Atom	*x*	*y*	*z*
Mo(1)	0.3916(2)	0.2614(1)	0.5602(1)
Mo(2)	0.2526(2)	0.3172(1)	0.4330(1)
Mo(3)	0.3033(2)	0.1554(1)	0.4374(1)
Mo(4)	0.1659(2)	0.2061(1)	0.5534(1)
Se(1)	0.1195(2)	0.1953(1)	0.4106(2)
Se(2)	0.3124(2)	0.1183(1)	0.5791(2)
Se(3)	0.2458(2)	0.3500(1)	0.5751(2)
Se(4)	0.4350(2)	0.2766(1)	0.4195(2)
O(1)	0.5458(12)	0.2092(9)	0.5799(9)
O(2)	0.5074(11)	0.3709(8)	0.5806(8)
O(3)	0.4154(12)	0.2709(9)	0.6878(9)
O(4)	0.1138(12)	0.3894(9)	0.4142(9)
O(5)	0.3338(12)	0.4403(9)	0.4146(9)
O(6)	0.2435(12)	0.3331(9)	0.3054(9)
O(7)	0.3065(12)	0.1383(9)	0.3086(9)
O(8)	0.4445(12)	0.0882(9)	0.4289(9)
O(9)	0.2321(12)	0.0273(9)	0.4251(9)
O(10)	0.0117(12)	0.2512(9)	0.5658(9)
O(11)	0.0561(12)	0.0927(8)	0.5610(8)
O(12)	0.1438(12)	0.2002(8)	0.6831(9)

atoms were refined with anisotropic thermal parameters, the C and O atoms with isotropic ones. Final *R* factors and other details are summarised in Table 3, positional parameters and selected bond distances and valence angles of the $[Mo_4Se_4(H_2O)_{12}]^{5+}$ cation in Tables 7 and 12.

Additional material available from the Cambridge Crystallographic Data Centre comprises remaining atomic coordinates, thermal parameters and remaining bond lengths and angles.

Infrared Spectra.[22]—Assignments to bridging ligands in the case of binuclear di-μ-oxo-dimolybdenum(v) complexing have been made by comparing spectra of ^{16}O- and ^{18}O-enriched forms.[23] Thus for such complexes only two of four vibrational modes from bridging ligands are observed, and prominent bands can be assigned in the 735–765 and 430–480 cm^{-1} regions.[24–27] Single μ-oxo-bridged complexes are characterised by a weak band at 754 ± 11 cm^{-1}, and di-μ-oxo systems by bands at 781 ± 1 and 712 ± 3 cm^{-1}.[23] On substituting one of the μ-oxo by a μ-sulfido a single band at 710 cm^{-1} due to the bridging Mo–O is observed. The di-μ-sulfido complex gives no bands in this region. In the present study tetramethylammonium salts of the thiocyanato complexes were prepared (as above), and spectra of KBr discs recorded on a Perkin Elmer 598 spectrometer. The only medium-to-weak bands in the 600–900 cm^{-1} range for $Mo_3O_3Se^{4+}$ and $Mo_3O_3S^{4+}$ can be assigned to bridging Mo–O stretching modes. Consideration of these and related complexes, Table 8, implicates Se as μ_3 and not a μ ligand.

Replacement of the bridging oxygen atoms by sulfur (or selenium) results in a shift in the Mo–O absorption frequency. This leads to a decrease in the splitting between the two bands, Table 8. Also a gradual decrease in intensity was observed in going from $Mo_3(\mu_3\text{-}X)(\mu\text{-}O)_3^{4+}$ to $Mo_3(\mu_3\text{-}X)(\mu\text{-}X)_3^{4+}$, where X = S or Se. A similar behaviour was observed for the μ-oxo–μ-sulfido-dimolybdenum(v) complexes.[22]

UV/VIS/NIR Spectra.—To avoid dissociation and hydrolysis processes of the aqua ions, acidic solutions, generally 2 M Hpts, were used. Spectra were recorded on a Perkin Elmer Lambda 9 instrument. For absorbance readings at < 300 nm, 2 M $HClO_4$

Table 8 Infrared Mo–O stretching bands (cm^{-1}) for trimolybdenum(IV) incomplete cuboidal oxosulfido $Mo_3O_xS_{4-x}^{4+}$ and oxoselenido $Mo_3O_xSe_{4-x}^{4+}$ (x = 0–4) clusters as thiocyanato complexes

Core cluster	
$Mo_3(\mu_3\text{-}O)(\mu\text{-}O)_3^{4+}$	720, 750, 775
$Mo_3(\mu_3\text{-}S)(\mu\text{-}O)_3^{4+}$	740, 765
$Mo_3(\mu_3\text{-}S)(\mu\text{-}O)_2(\mu\text{-}S)^{4+}$	740, 753
$Mo_3(\mu_3\text{-}S)(\mu\text{-}O)(\mu\text{-}S)_2^{4+}$	738
$Mo_3(\mu_3\text{-}S)(\mu\text{-}S)_3^{4+}$	No band(s) observed
$Mo_3(\mu_3\text{-}Se)(\mu\text{-}O)_3^{4+}$	740, 762
$Mo_3(\mu_3\text{-}Se)(\mu\text{-}O)_2(\mu\text{-}Se)^{4+}$	731, 744
$Mo_3(\mu_3\text{-}Se)(\mu\text{-}O)(\mu\text{-}Se)_2^{4+}$	726

Table 9 Selected bond distances (Å) and angles (°)* in $Na[NMe_4]\text{-}[Mo_2O_2Se_2(cys)_2]\cdot 7H_2O$

Mo–Mo^I	2.923(2)	Mo–O(2)	2.332(8)
Mo–Se	2.441(2)	Mo–N(1)	2.255(11)
Mo–Se^I	2.475(2)	S–C(3)	1.885(14)
Mo–S	2.489(3)	O(2)–C(1)	1.270(13)
Mo–O(1)	1.670(7)	N(1)–C(2)	1.528(16)
Se–Mo–Se^I	103.8(1)	S–Mo–O(2)	78.4(2)
Se–Mo–S	82.6(1)	S–Mo–N(1)	79.1(3)
Se–Mo–O(1)	106.5(3)	O(1)–Mo–O(2)	158.9(3)
Se–Mo–O(2)	92.8(2)	O(1)–Mo–N(1)	88.2(4)
Se–Mo–N(1)	157.5(3)	O(2)–Mo–N(1)	70.8(3)
Se^I–Mo–S	159.0(1)	Mo–Se–Mo^I	73.0(1)
Se^I–Mo–O(1)	101.8(4)	Mo–S–C(3)	101.1(4)
Se^I–Mo–O(2)	81.3(2)	Mo–O(2)–C(1)	114.3(7)
Se^I–Mo–N(1)	89.3(3)	Mo–N(1)–C(2)	107.3(7)
S–Mo–O(1)	95.3(3)		

* Symmetry transformation: I x, 1 − y, −z.

Table 10 Selected bond distances (Å) and angles (°) in $[NMe_4]_5\text{-}[Mo_3Se_4(NCS)_9]$

Mo(1)–Mo(2)	2.818(5)	Mo–(μ-Se)	
Mo(2)–Mo(3)	2.822(5)	Mo(1)–Se(2)	2.405(5)
Mo(1)–Mo(3)	2.811(6)	Mo(2)–Se(2)	2.402(6)
Mo–(μ_3-Se)		Mo(1)–Se(3)	2.399(6)
Mo(1)–Se(1)	2.454(6)	Mo(3)–Se(3)	2.409(6)
Mo(2)–Se(1)	2.444(5)	Mo(2)–Se(4)	2.417(6)
Mo(3)–Se(1)	2.460(6)	Mo(3)–Se(4)	2.424(5)
		Mo–N	2.19 (mean of 9)
Mo(2)–Mo(1)–Mo(3)	60.2(1)	(μ-Se)–Mo–(μ-Se)	
Mo(1)–Mo(2)–Mo(3)	59.8(1)	Se(2)–Mo(1)–Se(3)	94.2(2)
Mo(1)–Mo(3)–Mo(2)	60.0(1)	Se(2)–Mo(2)–Se(4)	92.5(2)
Mo–(μ_3-Se)–Mo		Se(3)–Mo(3)–Se(4)	94.4(2)
Mo(1)–Se(1)–Mo(2)	70.2(2)	(μ_3-Se)–Mo–N	83.5
Mo(1)–Se(1)–Mo(3)	69.8(2)		(mean of 6)
Mo(2)–Se(1)–Mo(3)	70.2(2)		159.4
(μ_3-Se)–Mo–(μ-Se)		(μ-Se)–Mo–N	(mean of 3)
Se(1)–Mo(1)–Se(2)	107.6(2)		88.8
Se(1)–Mo(1)–Se(3)	108.1(2)		(mean of 12)
Se(1)–Mo(2)–Se(2)	108.0(2)		164.8
Se(1)–Mo(2)–Se(4)	108.4(2)		(mean of 6)
Se(1)–Mo(3)–Se(3)	107.6(2)	N–Mo–N	80.4
Se(1)–Mo(3)–Se(4)	107.6(2)		(mean of 9)
Mo–(μ-Se)–Mo			
Mo(1)–Se(2)–Mo(2)	71.8(2)		
Mo(1)–Se(3)–Mo(3)	71.6(2)		
Mo(2)–Se(4)–Mo(3)	71.3(2)		

solutions were employed because of the strong absorption of Hpts in this region.

Cyclic Voltammetry.—Cyclic voltammograms were recorded on a Princeton Applied Research PAR 173 potentiostat interfaced to an Apple II Europlus microcomputer with a PAR 276 unit. The working electrode was a glassy carbon disc (Metrohm, diameter 2.5 mm). Platinum wire was used as a secondary electrode and a saturated calomel electrode was used as a reference.

Table 11 Selected bond distances (Å) and angles (°) in $[NMe_4]_5\text{-}[Mo_3O_2Se_2(NCS)_9]$

Mo(1)–Mo(2)	2.628(3)	Mo–(μ-O)	
Mo(1)–Mo(3)	2.628(3)	Mo(1)–O(1)	1.90(1)
Mo(2)–Mo(3)	2.802(4)	Mo(1)–O(2)	1.190(1)
Mo–(μ_3-Se)		Mo(2)–O(1)	1.90(1)
Mo(1)–Se(1)	2.469(3)	Mo(3)–O(2)	1.92(1)
Mo(2)–Se(1)	2.475(3)	Mo–N	2.15 (mean of 9)
Mo(3)–Se(1)	2.473(4)		
Mo–(μ-Se)			
Mo(2)–Se(2)	2.423(4)		
Mo(3)–Se(2)	2.422(3)		
Mo(2)–Mo(1)–Mo(3)	64.4(1)	(μ-Se)–Mo–(μ-O)	
Mo(1)–Mo(2)–Mo(3)	57.8(1)	Se(2)–Mo(2)–O(1)	95.9(4)
Mo(1)–Mo(3)–Mo(2)	57.8(1)	Se(2)–Mo(3)–O(2)	95.8(4)
Mo–(μ_3-Se)–Mo		(μ-O)–Mo–(μ-O)	
Mo(1)–Se(1)–Mo(2)	64.2(1)	O(1)–Mo(1)–O(2)	97.8(6)
Mo(1)–Se(1)–Mo(3)	64.3(1)	(μ_3-Se)–Mo–N	87.6 (mean of 6)
Mo(2)–Se(1)–Mo(3)	69.0(1)		
(μ_3-Se)–Mo–(μ-Se)			167.6
Se(1)–Mo(2)–Se(2)	107.3(1)		(mean of 3)
Se(1)–Mo(3)–Se(2)	107.5(1)	(μ-Se)–Mo–N	86.5
(μ_3-Se)–Mo–(μ-O)			(mean of 4)
Se(1)–Mo(1)–O(1)	103.0(4)		161.4
Se(1)–Mo(1)–O(2)	103.4(4)		(mean of 2)
Se(1)–Mo(2)–O(1)	102.7(4)	(μ-O)–Mo–N	86.6
Se(1)–Mo(3)–O(2)	102.6(4)		(mean of 8)
Mo–(μ-Se)–Mo			166.2
Mo(2)–Se(2)–Mo(3)	70.7(1)		(mean of 4)
Mo–(μ-O)–Mo		N–Mo–N	82.6
Mo(1)–O(1)–Mo(2)	87.3(6)		(mean of 9)
Mo(1)–O(2)–Mo(3)	86.9(6)		

Stability.—Solutions of the aqua ions $[Mo_3Se_4(H_2O)_9]^{4+}$, $[Mo_3OSe_3(H_2O)_9]^{4+}$ and $[Mo_3O_2Se_2(H_2O)_9]^{4+}$ in 2.0 M $HClO_4$ exhibited small (≈5%) irreversible spectrophotometric changes over 24 h in air. Such changes were more rapid, but were not quantified, in HCl. After 1–2 weeks in $HClO_4$ (or HCl) in air at 4 °C a deposit of red selenium was clearly visible. No change in spectrum was observed for solutions in 2.0 M $HClO_4$ stored under N_2 at ≈4 °C after 5 d. Similarly for solutions in 2 M Hpts at ≈4 °C no change in spectrum was observed after 2 weeks.

The $[Mo_4Se_4(H_2O)_{12}]^{5+}$ complex decomposes in air to give the trimolybdenum(IV) aqua ion $[Mo_3Se_4(H_2O)_9]^{4+}$, peaks at λ/nm 330 (sh), 425 and 648 at 25 °C for solutions in 2 M $HClO_4$ or Hpts. From absorbance changes over 20 h a half-life of ≈7 d was estimated at room temperature. For solutions in 2 M HCl changes occur more rapidly, half-life 20 h.

Results and Discussion

Structures.—Preparative procedures are summarised in Scheme 1. The structure of the dimolybdenum(V) complex $[Mo_2O_2(\mu\text{-}Se)_2(cys)_2]^{2-}$ **1** is shown in Fig. 3. Selected bond distances and angles are given in Table 9. The Mo–Mo distance of 2.92 Å compares with 2.83 Å for the di-μ-sulfido and 2.56 Å for the di-μ-oxo analogues. The di-μ-selenido like the di-μ-sulfido and di-μ-oxo complexes is diamagnetic, consistent with Mo–Mo bonding and with the yellow colour of the solution. The degree of folding of the Mo_2Se_2 ring, dihedral angle 31°, is similar to that observed in the oxo and sulfido analogues and allows a closer approach of the two Mo, as does the Mo–Se–Mo angle of 73°. Also the angles O(1)–Mo–Se(Se^I) (104.1°) and Se–Mo–Se^I (103.8°) are relevant to the Mo–Mo interaction.

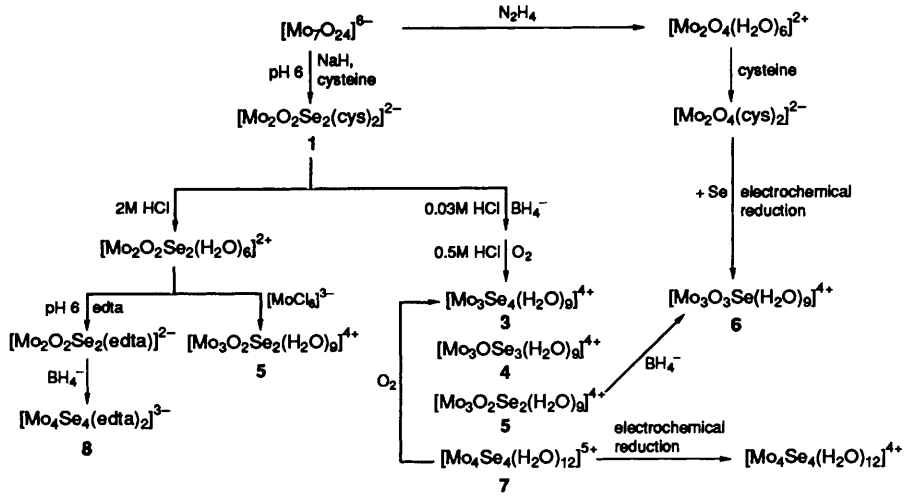

Scheme 1

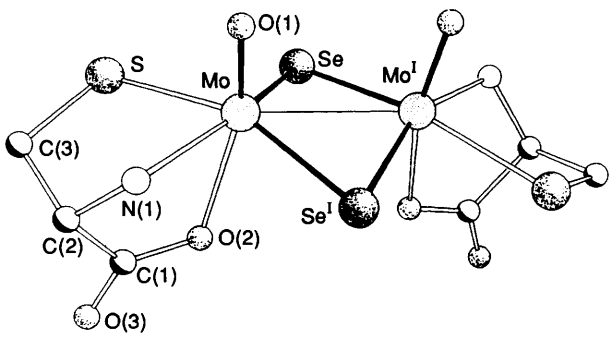

Fig. 3 Structure of $[Mo_2O_2(\mu\text{-}Se)_2(cys)_2]^{2-}$ **1** showing the atom labelling scheme

These various distortions give a structure which can be described as seven-co-ordinate capped octahedral, with a bent Mo–Mo bond in the seventh co-ordination position.

The structural features of the NMe_4^+ salts of the thiocyanato complexes of $Mo_3Se_4^{4+}$ (**3**) and $Mo_3O_2Se_2^{4+}$ (**5**), Fig. 4, confirm the trends observed for the oxo and sulfido analogues, with the Mo–Mo distances 2.82 Å for **3**, and different values (according to the chemical nature of the bridges), 2.80 and 2.63 Å, in **5**. The $Mo_3O_4^{4+}$ core is crystallographically well characterised (seven structures).[7] The Mo–Mo distance is close to 2.50 Å, consistent with metal–metal bonding, and Mo–μ_3-O (2.03 Å) is longer than the Mo–μ-O bond (1.92 Å). For the $Mo_3S_4^{4+}$ core the Mo–Mo distance is 2.76 Å, with smaller differences between the Mo–μ_3-S (2.34) and Mo–μ-S (2.29 Å) bond distances (average of 31 structures).[7] The Mo–μ_3-Se (2.45) and Mo–μ-Se (2.41 Å) bond lengths are consistent with the 0.14 Å larger ionic radius of selenide compared with sulfide. Also, the bond angles at the chalcogen bridges show a clear correlation to the size of the chalcogen. The Mo–μ_3-Se–Mo angles of 70.1° in $Mo_3Se_4^{4+}$ and of 69.0 and 64.3° in $Mo_3O_2Se_2^{4+}$ as well as the Mo–μ-Se–Mo values of 71.6 ($Mo_3Se_4^{4+}$) and 70.7° ($Mo_3O_2Se_2^{4+}$) (Tables 10 and 11) are systematically smaller than the average values of 76 (Mo–μ_3-O–Mo) and 81° (Mo–μ-O–Mo) in $Mo_3O_4^{4+}$, or of 72 (Mo–μ_3-S–Mo) and 74° (Mo–μ-S–Mo) in $Mo_3S_4^{4+}$.[7]

The structure of the pts^- salt of the 5+ cube cluster **7** as the aqua ion is shown in Fig. 5, with selected bond lengths and angles in Table 12. The mean Mo–Mo distance of 2.866 Å compares with 2.802 Å observed for $[Mo_4S_4(H_2O)_{12}]^{5+}$.[7] The difference here of 0.064 Å is very similar to the 0.060 Å indicated for the trinuclear selenium and sulfur analogues. The same is true for the Mo–μ_3-Se bond lengths of 2.480 Å (average) Table 13, which differ from the values for Mo–μ_3-S in $Mo_4S_4^{5+}$ cores

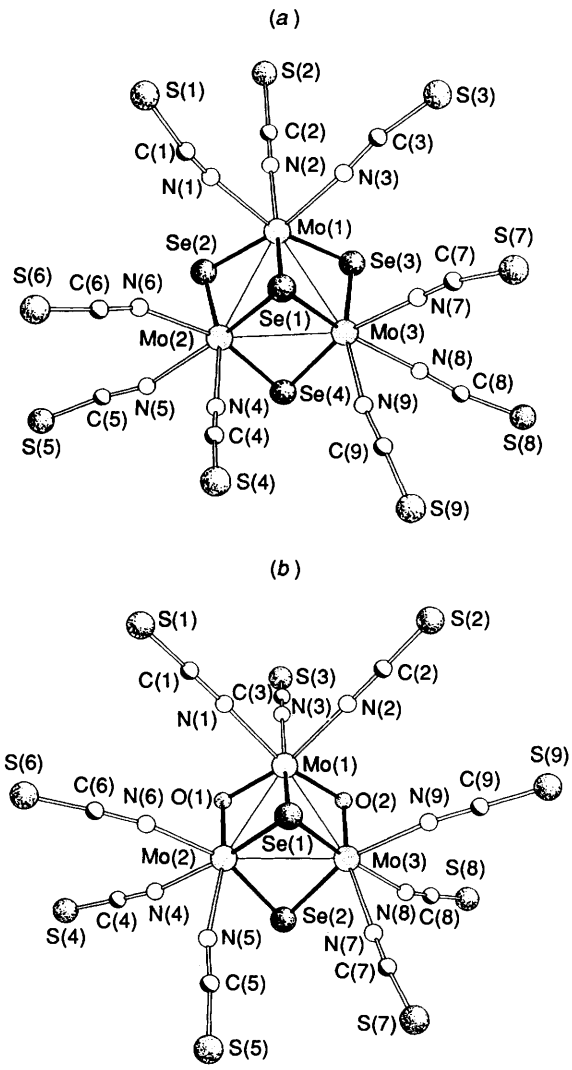

Fig. 4 Structures of $[Mo_3(\mu_3\text{-}Se)(\mu\text{-}Se)_3(NCS)_9]^{5-}$ (*a*) and $[Mo_3(\mu_3\text{-}Se)(\mu\text{-}O)_2(\mu\text{-}Se)(NCS)_9]^{5-}$ (*b*) showing the atom labelling scheme

(average 2.35 Å) by the difference in the ionic radii of S^{2-} and Se^{2-}. The four Mo's have 11 electrons, one less than is required to give six Mo–Mo bonds, and both the $[Mo_4Se_4(H_2O)_{12}]^{5+}$ and $[Mo_4S_4(H_2O)_{12}]^{5+}$ ions give EPR spectra with no evidence of hyperfine structure in support of the localised

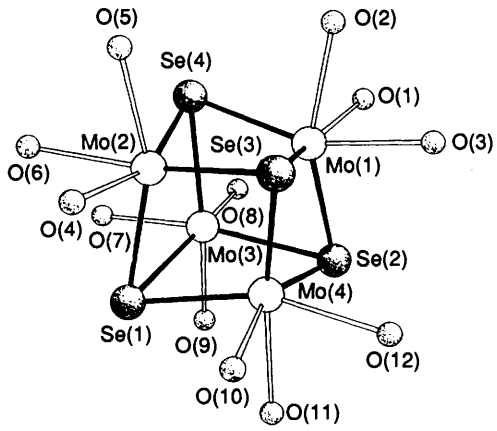

Fig. 5 Structure of $[Mo_4Se_4(H_2O)_{12}]^{5+}$ **7**, showing the atom labelling scheme

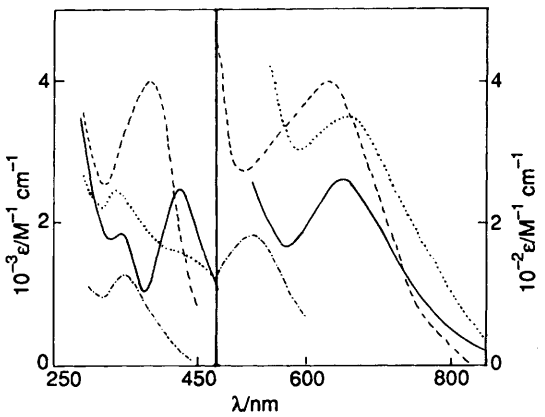

Fig. 6 The UV/VIS absorption spectra of trimolybdenum(IV) aqua ion clusters $Mo_3Se_4^{4+}$ **3** (——), $Mo_3OSe_3^{4+}$ **4** (– – –), $Mo_3O_2Se_2^{4+}$ **5** (– · – · –) and $Mo_3O_3Se^{4+}$ **6** (· · · ·) in 2 M Hpts, ε values per trinuclear complex

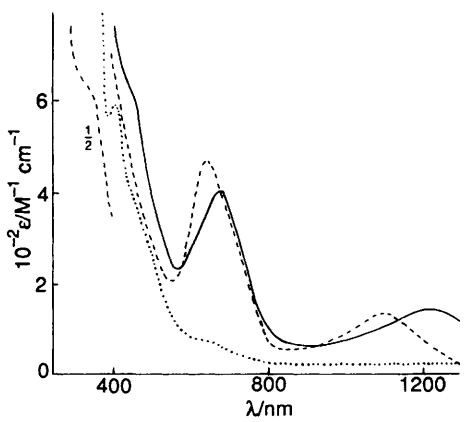

Fig. 7 The UV/VIS absorption spectra of $[Mo_4Se_4(H_2O)_{12}]^{5+}$ **7** (——), $[Mo_4Se_4(H_2O)_{12}]^{4+}$ (· · ·), and for comparison the $[Mo_4S_4(H_2O)_{12}]^{5+}$ (– – –) analogue in 2 M Hpts, ε values per cube. The 4+ spectrum includes a small contribution from 5+ at ≈ 660 nm

structure.[30,31] Note however that kinetic studies on the NCS^- complexing with $[Mo_4S_4(H_2O)_{12}]^{5+}$ provide evidence for two different oxidation states.[30]

UV/VIS Absorption Bands.—Spectra of the four trinuclear $[Mo_3O_xSe_{4-x}(H_2O)_9]^{4+}$ clusters are shown in Fig. 6. Charge-transfer bands are observed in the 634–660 nm range for the three μ-Se containing clusters, whereas the μ_3-Se cluster $[Mo_3O_3Se(H_2O)_9]^{4+}$ has a less strong peak at 525 nm. Similar

Table 12 Selected distances (Å) and angles (°) in $[Mo_4Se_4(H_2O)_{12}][MeC_6H_4SO_3]_5\cdot 14H_2O$

Mo(1)–Mo(2)	2.918(4)	Mo(2)–Se(4)	2.480(4)
Mo(1)–Mo(3)	2.816(4)	Mo(3)–Se(1)	2.492(4)
Mo(1)–Mo(4)	2.890(4)	Mo(3)–Se(2)	2.478(4)
Mo(2)–Mo(3)	2.791(4)	Mo(3)–Se(4)	2.482(4)
Mo(2)–Mo(4)	2.916(4)	Mo(4)–Se(1)	2.462(4)
Mo(3)–Mo(4)	2.862(4)	Mo(4)–Se(2)	2.478(4)
Mo(1)–Se(2)	2.478(4)	Mo(4)–Se(3)	2.485(4)
Mo(1)–Se(3)	2.480(4)	Mo–O	
Mo(1)–Se(4)	2.480(4)	range	2.17(2)–2.23(2)
Mo(2)–Se(1)	2.485(4)	mean of 12	2.199
Mo(2)–Se(3)	2.475(4)		
Mo–Mo–Mo		O–Mo–O	
range	57.8(1)–62.7(1)	range	75.4(5)–79.6(5)
mean of 12	60	mean of 12	77.5
Se–Mo–Se		Se–Mo–O	
range	104.1(1)–109.5(1)	mean of 12	158.6
mean of 12	106.4	mean of 24	86.0
Mo–Se–Mo			
range	68.2(1)–72.2(1)		
mean of 12	70.6		

Table 13 Summary of bond lengths (Å) obtained in this work for Mo–Se clusters

	Average	
Complex	Mo–μ-Se	Mo–μ_3-Se
$[Mo_2O_2Se_2(cys)_2]^{2-}$	2.458	—
$[Mo_3Se_2O_2(NCS)_9]^{5-}$	2.419	2.473
$[Mo_3Se_4(NCS)_9]^{5-}$	2.411	2.451
$[Mo_4Se_4(H_2O)_{12}]^{5+}$	—	2.480

trends are observed for the $[Mo_3O_xS_{x-4}(H_2O)_9]^{4+}$ series, with μ-S containing cores giving a 572–602 nm range of values, and the μ_3-S cluster $[Mo_3O_3S(H_2O)_9]^{4+}$ a less-intense peak at 512 nm.[12] Interestingly the μ_3-O containing $[Mo_3O_4(H_2O)_9]^{4+}$ cluster has a peak at 505 nm. In all cases the peaks are broad, and the ordering of wavelength maxima $Mo_3S_4^{4+}$ > $Mo_3OS_3^{4+}$ > $Mo_3O_2S_2^{4+}$, but $Mo_3OSe_3^{4+}$ > $Mo_3Se_4^{4+}$ > $Mo_3O_2Se_2^{4+}$, suggests that the envelope includes more than one transition. What is clear is that there is a red shift on replacing S with Se which for the μ_2 core ligands is 60 nm and for μ_3 is considerably less at 13 nm. Bands at < 425 nm give a less clear-cut pattern, and other transitions may be involved. The $[Mo_4Se_4(H_2O)_{12}]^{5+}$ cube, with μ_3-Se core ligands only, exhibits a small red shift, 662 nm, as compared to 645 nm for $[Mo_4S_4(H_2O)_{12}]^{5+}$, Fig. 7, consistent with the above trends. The transition is associated with the molybdenum(IV) component since the 4+ Mo^{IV}_4 cubes have no clearly defined peak in this region and indeed have only a shoulder at 450 nm.

No bands are observed in the NIR for the trimolybdenum(IV) clusters. In the case of $[Mo_4Se_4(H_2O)_{12}]^{5+}$ the band at 1188 nm (ε 117 $M^{-1}\,cm^{-1}$) is comparable to that of $[Mo_4S_4(H_2O)_{12}]^{5+}$ at 1100 nm (ε 122 $M^{-1}\,cm^{-1}$). The edta complexes have corresponding peaks at 1210 (190) for $[Mo_4Se_4(edta)_2]^{3-}$ and 1145 nm (280 $M^{-1}\,cm^{-1}$) for $[Mo_4S_4(edta)_2]^{3-}$, Fig. 8. The most likely interpretation is in terms of intervalence charge-transfer bands.

On replacing S by Se in [2Fe–2S] proteins absorption bands at ≈420 and 460 nm have been observed to undergo red shifts of 20 nm.[5] In contrast the band at *ca.* 330 nm remains unchanged, and it has been suggested that this arises mainly from (Cys)S→Fe charge transfer.[32–35] Similar shifts for binuclear complexing have been observed.[1,3]

For the [4Fe–4S] proteins, shifts in the bands at 300 and

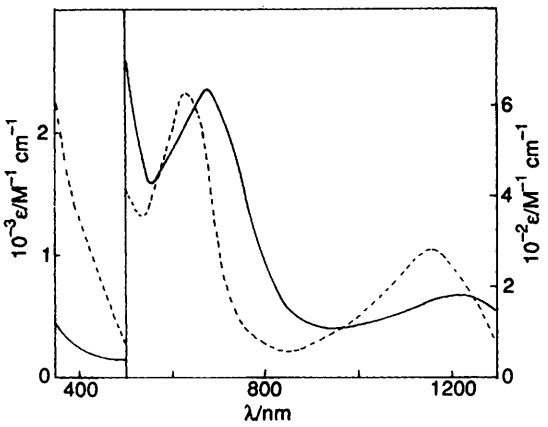

Fig. 8 The UV/VIS absorption spectra of $[Mo_4Se_4(edta)_2]^{3-}$ **8** (——) alongside $[Mo_4S_4(edta)_2]^{3-}$ (– – – –) in 0.5 M $LiClO_4$, ε values per cube

400 nm upon selenium substitution are hardly detectable or ill defined.[36] The most likely reason is that transitions involving Se and S to Fe and (Cys)S→Fe charge transfers overlap.[37] Well characterised red shifts have only been observed for the cuboidal cluster having aromatic ligands. In this case the shifts are variable, as expected for clusters having RS ⟶ Fe transitions close to the visible absorption maximum at 450 nm.[38] In CD and MCD spectra of Se-substituted [4Fe–4S] proteins the peaks are also shifted to lower energies.[39]

Reduction Potentials.—Cyclic voltammograms for one-electron reduction and oxidation processes of $[Mo_4Se_4(H_2O)_{12}]^{5+}$ (3 mM) in 2.0 M Hpts are shown in Fig. 9. Both processes exhibit reversible behaviour, and analysis of the one-electron waves gives $E_{pc,1} = -0.084$ V, $E_{pa,1} = -0.012$ V and $E_{pc,2} = 0.516$ V, $E_{pa,2} = 0.586$ V. From these values reduction potentials (± 5 mV) for equations (1) and (2), both *vs.* the normal hydrogen electrode, were obtained.

$$[Mo_4Se_4(H_2O)_{12}]^{5+} + e^- \rightleftharpoons [Mo_4Se_4(H_2O)_{12}]^{4+} \quad (0.190\ V) \quad (1)$$

$$[Mo_4Se_4(H_2O)_{12}]^{6+} + e^- \rightleftharpoons [Mo_4Se_4(H_2O)_{12}]^{5+} \quad (0.790\ V) \quad (2)$$

With $[Mo_4Se_4(edta)_2]^{3-}$ (2 mM) in 0.50 M $LiClO_4$ as the starting complex, cyclic voltammograms show quasi-reversible one-electron reduction and oxidation, Fig. 10. Analysis of the one-electron waves gives $E_{pc,1} = -0.322$ V, $E_{pa,1} = -0.240$ V and $E_{pc,2} = 0.378$ V, $E_{pa,2} = 0.440$ V. These gave reduction potentials (*vs.* NHE) as indicated in equations (3) and (4).

$$[Mo_4Se_4(edta)_2]^{3-} + e^- \rightleftharpoons [Mo_4Se_4(edta)_2]^{4-} \quad (-0.040\ V) \quad (3)$$

$$[Mo_4Se_4(edta)_2]^{2-} + e^- \rightleftharpoons [Mo_4Se_4(edta)_2]^{3-} \quad (0.650\ V) \quad (4)$$

Errors in these determinations are estimated as ± 0.005 V. The effects of replacing S by Se can be summarised as a shift in reduction potentials to less-positive values for the aqua ions 5+/4+ (20 mV) and 6+/5+ (70 mV), whereas with edta as ligand no changes were detected, Table 14. Positive shifts of 0–60 mV are observed for both [2Fe–2S][3] and [4Fe–4S],[2] synthetic analogues. In the case of proteins the effects are more variable however, and are not always positive.[35,37,40–42] To some extent these inconsistencies may arise from the lack of accuracy in measurements. The effect of polypeptide chains may also be important.[5] Overall it appears that there is no set pattern or trend of reduction potentials on replacing S by Se.

Table 14 A comparison of reduction potentials (E_f° *vs.* NHE) of aqua (2.0 M Hpts) and edta complexes (0.5 M $LiClO_4$) of Mo_4Se_4 and Mo_4S_4 cuboidal clusters at 22 °C.

	E_f°/V	
Couple	X = Se	S
$[Mo_4X_4(H_2O)_{12}]^{5+/4+}$	0.19	0.21
$[Mo_4X_4(H_2O)_{12}]^{6+/5+}$	0.79	0.86
$[Mo_4X_4(edta)_2]^{3-/4-}$	−0.040	−0.046
$[Mo_4X_4(edta)_2]^{2-/3-}$	0.65	0.65

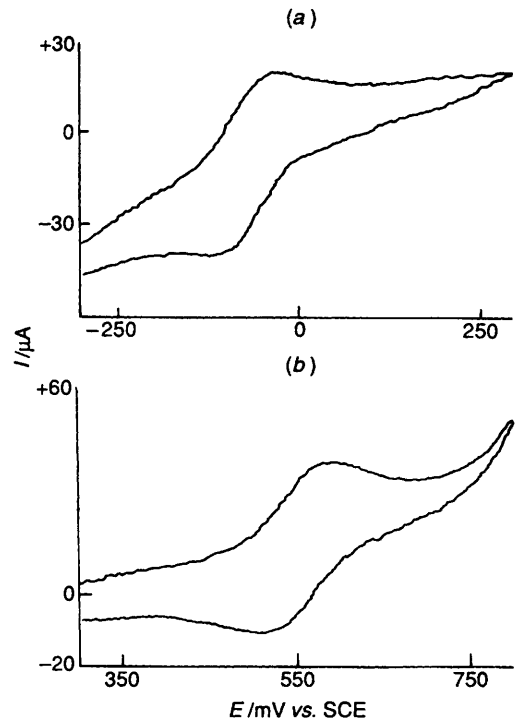

Fig. 9 Cyclic voltammograms of $[Mo_4Se_4(H_2O)_{12}]^{5+}$ **7** (3 mM) in 2.0 M Hpts, scan rate 100 mV s^{-1}, corresponding to redox changes of (*a*) 5+/4+ and (*b*) 6+/5+

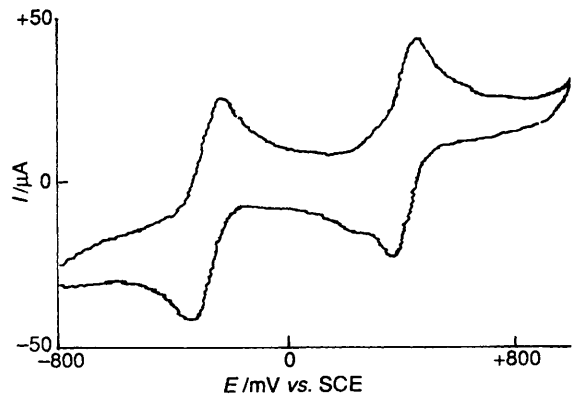

Fig. 10 Cyclic voltammogram of $[Mo_4Se_4(edta)_2]^{3-}$ (2 mM) in 0.5 M $LiClO_4$, scan rate 100 mV s^{-1} corresponding to 5+/4+ and 6+/5+ redox changes

Formation of Mixed-metal Cubes.—By analogy with $[Mo_3S_4(H_2O)_9]^{4+}$, rigorously air-free yellow-brown solutions of $[Mo_3Se_4(H_2O)_9]^{4+}$ (0.5 mM, 20 cm^3) in 1 M HCl react readily with selected metals. Thus with iron wire (0.5 g, Johnson Matthey Spec pure) a red solution was obtained within 4 h. The corresponding reaction with copper turnings (0.5 g, BDH),

which was much faster (≈1 h), also resulted in a red solution. The analogous reaction with mercury gave a green solution after 2 h. Absorption coefficients were determined by air oxidation of the cube to give trinuclear $[Mo_3Se_4(H_2O)_9]^{4+}$ the spectrum of which is known. The same products were obtained by reaction of metal salts with BH_4^- as reductant. The analogous products obtained from $[Mo_3S_4(H_2O)_9]^{4+}$ have been shown by crystallography to have a single cube, $[Mo_3FeS_4(H_2O)_{10}]^{4+}$, an edge-shared double cube, $[\{Mo_3CuS_4(H_2O)_9\}_2]^{8+}$, and a corner-shared double cube $[Mo_3S_4HgS_4Mo_3(H_2O)_{18}]^{8+}$ structure.[7] These observations indicate the potential for a whole new area of heterometal cluster chemistry.

Acknowledgements

We thank the UK Science and Engineering Research Council for a research grant (to M. N. and G. J. L.) and Laporte Industries for a CASE studentship (to C. A. R.). G. J. L. is also grateful to the University of the Orange Free State in Bloemfontein for leave of absence. G. H. and B. K. thank the Fonds der Chemischen Industrie and the Bundesminister für Forschung und Technologie (BMFT) for financial support.

References

1 S.-B. Yu, G. C. Papaefthymiou and R. H. Holm, *Inorg. Chem.*, 1991, **30**, 3476.
2 M. A. Bobrik, E. J. Laskowski, R. W. Johnson, W. O. Gillum, J. M. Berg, K. O. Hodgson and R. H. Holm, *Inorg. Chem.*, 1978, **17**, 1402.
3 J. G. Reynolds and R. H. Holm, *Inorg. Chem.*, 1980, **19**, 3257.
4 M. A. Greaney, C. L. Coyle, R. S. Pilato and E. I. Stiefel, *Inorg. Chim. Acta*, 1991, **189**, 81.
5 J. Meyer, J.-M. Moulis, J. Gaillard and M. Lutz, *Adv. Inorg. Chem.*, 1992, **38**, 73.
6 T. C. Stadtman, *Annu. Rev. Biochem.*, 1990, **59**, 111.
7 T. Shibahara, *Adv. Inorg. Chem.*, 1991, **37**, 143.
8 R. H. Holm, *Adv. Inorg. Chem.*, 1992, **38**, 1.
9 B.-L. Ooi, C. Sharp and A. G. Sykes, *J. Am. Chem. Soc.*, 1989, **111**, 125.
10 C. Sharp and A. G. Sykes, *J. Chem. Soc., Dalton Trans.*, 1988, 2579.
11 B.-L. Ooi and A. G. Sykes, *Inorg. Chem.*, 1989, **28**, 3799.
12 M. Martinez, B.-L. Ooi and A. G. Sykes, *J. Am. Chem. Soc.*, 1987, **109**, 4615.
13 R. H. Holm, S. Ciurli and J. A. Weigel, *Prog. Inorg. Chem.*, 1990, **38**, 18.
14 K. S. Hagen, A. D. Watson and R. H. Holm, *J. Am. Chem. Soc.*, 1983, **105**, 3905.
15 G. Henkel, G. Kampmann, B. Krebs, G. J. Lamprecht, M. Nasreldin and A. G. Sykes, *J. Chem. Soc., Chem. Commun.*, 1990, 1014.
16 S. Harris, *Polyhedron*, 1989, **8**, 2843.
17 See, for example, P. W. Dimmock, D. P. E. Dickson and A. G. Sykes, *Inorg. Chem.*, 1990, **29**, 5120.
18 Q.-T. Liu, J.-X. Lu and A. G. Sykes, *Inorg. Chim. Acta*, 1992, **198–200**, 623.
19 A. Kay and P. C. H. Mitchell, *J. Chem. Soc. A*, 1970, 2421.
20 SHELXTL+ program package, Siemens Analytical X-ray Instruments, Madison, WI.
21 *International Tables for X-Ray Crystallography*, Kynoch Press, Birmingham, 1974, vol. 4.
22 V. R. Ott, D. S. Swieter and F. A. Schultz, *Inorg. Chem.*, 1977, **16**, 2538.
23 W. E. Newton and J. W. McDonald, *Proceedings of the Second International Conference on the Chemistry and Uses of Molybdenum*, ed. P. C. H. Mitchell, Climax Molybdenum, London, 1976, p. 25; *J. Less-Common Met.*, 1977, **54**, 51.
24 L. R. Melby, *Inorg. Chem.*, 1969, **8**, 349.
25 W. E. Newton, J. L. Corbin, D. C. Bravard, J. E. Searles and J. W. McDonald, *Inorg. Chem.*, 1974, **13**, 1100.
26 W. E. Newton, J. L. Corbin and J. W. McDonald, *J. Chem. Soc., Dalton Trans.*, 1974, 1044.
27 B. Jezowska-Trzebiatowska, M. F. Rudolf, L. Natkaniec and H. Sabat, *Inorg. Chem.*, 1974, **13**, 617.
28 D. H. Brown and J. A. D. Jeffreys, *J. Chem. Soc., Dalton Trans.*, 1973, 732.
29 J. R. Knox and C. K. Prout, *Acta Crystallogr., Sect. B*, 1969, **25**, 1857.
30 M. Nasreldin, Y.-J. Li, M. Humanes and A. G. Sykes, *Inorg. Chem.*, 1992, **31**, 3011.
31 P. W. Dimmock, J. McGinnis, B.-L. Ooi and A. G. Sykes, *Inorg. Chem.*, 1990, **29**, 1085.
32 J. C. M. Tsibris, M. J. Namtvedt and I. C. Gunsalus, *Biochem. Biophys. Res. Commun.*, 1968, **3**, 323.
33 W. H. Orme-Johnson, R. E. Hansen, H. Beinert, J. C. M. Tsibris, R. C. Bartholomaus and I. C. Gunsalus, *Proc. Natl. Acad. Sci. USA*, 1968, **60**, 368; K. Mukai, J. J. Huang and T. Kimura, *Biochem. Biophys. Res. Commun.*, 1973, **50**, 105.
34 J. A. Fee and G. Palmer, *Biochim. Biophys. Acta*, 1971, **245**, 175, 196.
35 J. Meyer, J.-M. Moulis and M. Lutz, *Biochim. Biophys. Acta*, 1986, **871**, 243.
36 J.-M. Moulis, M. Lutz, J. Gaillard and L. Noodleman, *Biochemistry*, 1988, **27**, 8712.
37 J.-M. Moulis and J. Meyer, *Biochemistry*, 1982, **21**, 4762.
38 J.-M. Moulis, J. Meyer and M. Lutz, *Biochemistry*, 1984, **23**, 6605.
39 S. J. George, A. J. Thompson, D. E. Crabtree, J. Meyer and J.-M. Moulis, *New. J. Chem.*, 1991, **15**, 455.
40 J. A. Fee, S. G. Mayhew and G. Palmer, *Biochim. Biophys. Acta*, 1971, **245**, 196.
41 G. S. Wilson, J. C. M. Tsibris and I. C. Gunsalus, *J. Biol. Chem.*, 1973, **248**, 6059.
42 K. Mukai, J. J. Huang and T. Kimura, *Biochim. Biophys. Acta*, 1974, **336**, 427.

Received 22nd *October* 1992; *Paper* 2/05648H